

High resolution ultrasound in entrapment neuropathies

PhD thesis

Dr. Csillik Anita

Semmelweis University Szentágothai János School of PhD Studies in
Neuroscience



Consultant: Zsuzsanna Arányi, MD, DSc

Referees: Károly Altdorfer, MD, PhD
Klára Fekete MD, PhD

Chairman for PhD examination: Professor István Bitter, MD, DSc.
Comittee for PhD examination: Zoltán Hidasi, MD, PhD
Anna Kelemen, MD, PhD

Budapest
2019

INTRODUCTION

Compressive neuropathies are the most common forms of peripheral neuropathies. Electrodiagnostic studies, which assess the degree of functional loss have been widely regarded as the „gold standard” method for diagnosis. The introduction of high resolution ultrasonography (HRUS) gave an opportunity to visualize these conditions, and to examine the structural appearance of peripheral nerves at the fascicular level. HRUS has recently emerged as an easily available and reliable tool in the diagnostic workup of various entrapment neuropathies.

Pathophysiological events that are initiated by the increased pressure in entrapment neuropathies have well defined sonographic correspondances: 1. the nerve becomes hypoechoic proximal and distal to the site of compression, 2. there is a segmental enlargement of the cross-sectional area (CSA), 3. on longitudinal scans there is an abrupt caliber drop at the site of compression and a spindle-like segmental swelling of the nerve proximal and distal to it; these changes are defined by the longitudinal anteroposterior diameter (LAPD).

Idiopathic carpal tunnel syndrome (CTS) is the most common peripheral entrapment neuropathy. It is caused by compression of the median nerve by the flexor retinaculum at the wrist within the carpal tunnel, leading to pain, sensorimotor deficit and dysfunction of the hand. Electrodiagnostic confirmation is the main choice. From the 1990's on high resolution ultrasonography (HRUS) has emerged as a complementary tool in the assessment of CTS, with a diagnostic sensitivity of 44-95%, and a specificity of 57-100%. In about 10-25 % of the cases, when electrodiagnostic studies are negative or not confirmatory, ultrasound has an even more pronounced utility.

In CTS compression leads to flattening of the median nerve in the tunnel, endoneurial edema, perineurial and endoneurial thickening with consequent hypoechoicity and nerve enlargement on ultrasound. The so called ‘notch sign’ is a typical finding on longitudinal scans, which occurs as a consequence of the abrupt caliber drop at the site of compression. Nerve swelling is found proximal and distal to the compression. The meta-analyses of the large body of literature concluded that level A evidence support the ultrasonographic measurement of median nerve cross-sectional area at the tunnel inlet (CSA-I) as an accurate diagnostic test for CTS. Most of the articles concluded that $CSA-I \geq 9 \text{ mm}^2$ provides the highest sensitivity and specificity (87.3% and 83.3%, respectively). Furthermore the use of the wrist-to-forearm ratio (WFR) was also proposed, with $WFR \geq 1,4$ giving a sensitivity of 100% in this patient sample.

The second most common entrapment neuropathy after carpal tunnel syndrome is ulnar neuropathy at the elbow (UNE). The most frequent form is the true cubital tunnel syndrome, in which compression is caused by the thick aponeurosis covering between the two heads of flexor carpi ulnaris muscle. Typical clinical signs involve numbness, paraesthesia of the 4-5. fingers, and paresis and atrophy of the ulnar innervated muscles. The major limitation of electrodiagnostic evaluation of UNE occurs in cases of pure axonal damage, when it fails to localize the site of the lesion. As HRUS has the advantage to localize the lesion, it gained a considerable role in the diagnosis. With the use of relevant parameters HRUS is regarded to have a sensitivity of 80%-100 %, and a specificity of 90% in UNE. It has an even more significant role in less severe cases, when electrodiagnostic studies are yet negative. Sonodiagnosis is based on the maximal CSA and LAPD values. Moreover the cubital-to-humeral nerve area ratio (CHR), i.e. the swelling ratio also proved to be an important parameter in establishing diagnosis. The combination of complete fascicular masking and a CHR more than 1,4 was proposed as the best US parameter for UNE.

Posteromedial tarsal tunnel syndrome is a rare entrapment neuropathy which is caused by the compression of the posterior tibial nerve or its branches in the fibrous osseous tarsal tunnel. Typical complaints are burning pain and paraesthesia affecting the heel or sole triggered by walking. HRUS has been proposed to be a routine element for the diagnosis, since in most of the cases the enlarged nerve or the compressive cause (e.g. varicose plantar veins or an accessory muscle belly) can be identified.

Thoracic outlet syndrome constitute another rare entity among entrapment neuropathies. It is characterized by compression of the brachial plexus or the subclavian vessels at any point in the thoracic outlet region. In neurogenic TOS, the brachial plexus is typically compressed in the scalenic triangle at the level of the lower trunk or the distal portion of its constituents, the C8 and Th1 anterior primary rami (roots). This gives rise to a characteristic clinical syndrome with selective wasting of the thenar and the first dorsal interosseus muscle with sensory disturbance and pain on the medial aspect of the forearm. The electrophysiologic hallmark of neurogenic TOS is the demonstration of post-ganglionic sensorimotor C8–Th1 axon loss, with Th1 being more affected. The category nonspecific TOS is a controversial category with a lack of consensus on its etiology and pathomechanism. It is characterized by subjective symptoms such as pain and paresthesia in the arm especially when lifted overhead, with no clinical deficit.

AIMS

Although, the swelling of the median nerve (or generally any nerve under compression) may occur both proximally and distally to the compression, to date very little attention has been paid to measurements at the carpal tunnel outlet on the palm. In our routine work it was our observation that in most CTS patients the swelling was conspicuous and often even more pronounced or isolated at the tunnel outlet on the palm than at the inlet at the wrist. Moreover, it was our impression that the degree of flattening of the median nerve within the carpal tunnel was usually the greatest in the distal tunnel and that the greater the distal flattening was, the greater was the swelling at the outlet. Our aim was to statistically analyze these observations and to test our hypothesis that the pronounced swelling at the outlet is related to increasing compression from proximal to distal in the tunnel. Our further purpose was to prove the value of sonographic outlet measurements in CTS patients who showed no electrophysiological deficit.

Sonographic findings typical for entrapment neuropathies may overlap with those of other peripheral nerve disorders, such as tumours and neuromas, and may cause differential diagnostic problems, especially if the enlargement is of unusually large degree. Our aim was to highlight that in rare cases an unusual degree of nerve swelling may occur in entrapment neuropathies. We present three cases of entrapment neuropathies where tumour-like giant nerves were observed.

The pathognomic role of the fibromuscular ligaments in TOS was originally identified by Roos and Brantigan based on their surgical and cadaveric studies. As a modern imaging technique HRUS is a suitable tool for a possible pre-surgical detection, but despite of its ease and accessibility, data in the literature regarding the use of HRUS in the diagnosis of TOS is insignificant. Our aim was to present a consecutive case series of patients with neurogenic and nonspecific TOS assessed by HRUS.

METHODS

All patients underwent clinical, electrophysiologic and ultrasound assessments. Most of the electrodiagnostic and neurosonographic studies were performed at our laboratory at the Neurological Department of Semmelweis University using the Nicolet Viking Quest or EDX System (CareFusion Corporation, a Philips Epiq 5 device with a 18- to 5-MHz linear array transducer, manufactured by Philips (Amsterdam, Netherlands) and A Philips HD15 XE Pure Wave device with a 12- to 5-MHz 50-mm linear array transducer. Settings were optimized for

nerve imaging, including the use of compound imaging mode. For CTS 118 hands of 87 patients were assessed in a retrospective study. Inclusion criteria were the typical clinical symptoms and signs of idiopathic CTS and its electrophysiological confirmation. A control group was also examined, including 44 hands of 23 individuals. Another group of 10 patients (12 hands) with typical CTS symptoms but showing no electrophysiological deficit were also assessed in a second session. Ultrasonographic CSA measurements were made at the tunnel inlet (CSA-I), at the tunnel outlet (CSA-O) and at the forearm. Two parameters, the wrist-to-forearm ratio (WFR) and the palm-to-forearm ratio (PFR) of the CSA values were calculated. On longitudinal scans LAPDs were measured at four points (Fig. 1). Statistical analysis was performed by using Statistica for Windows v.12 program (StatSoft Tulsa OK. USA) and online statistical calculators (<http://www.socscistatistics.com/tests>, <http://www.rad.jhmi.edu/jeng/javarad/roc/JROCFITi.html>, https://www.medcalc.org/calc/diagnostic_test.php) with the significance level set at $p < 0.05$. Age, CSA-I, CSA-O, WFR, PFR and LAPD values were described by descriptive statistics. Depending on normality, unpaired t-test or Mann–Whitney U test was used to compare parameters between the control and patient groups, and the Paired t-test or Wilcoxon matched pairs signed rank test was used to perform comparisons within a group. The cut-off values with the highest sensitivity and specificity for cross sectional parameters were determined by receiver operating characteristic (ROC) analysis, and the sensitivity, specificity, positive and negative predictive values and accuracy of these parameters and their combinations in CTS were calculated.

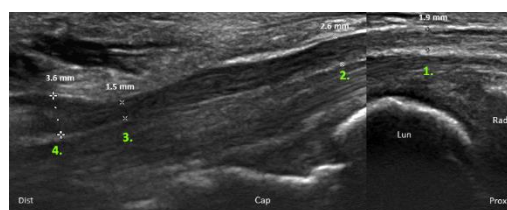


Fig. 1. LAPD measurements at 4 points in the carpal tunnel

In order to demonstrate unusual tumor-like nerve enlargement in entrapment neuropathies we examined a 60 year old woman and a 67 year old man with clinical symptoms of ulnar nerve deficit and a 62 year old woman with the diagnosis of bilateral tarsal tunnel syndrome. On ultrasonographic assessment we measured the maximal CSA (CSA_{max}) both in the cubital and tarsal tunnel, regarding the ulnar nerve we calculated the CHR value.

On longitudinal scans the maximal LAPDs were measured at the maximal width both in the cubital and the tarsal tunnel. We have conducted a retrospective analysis of the ultrasonographic measurements of 47 (50 arms) consecutive patients with electrophysiologically diagnosed cubital tunnel syndrome, the CSA_{max}, CHR and LAPD_{max} values were described by descriptive statistics.

For TOS assessments twenty consecutive patients were included in the retrospective analysis. 15 patients were diagnosed with neurogenic TOS, all of them showed clinical symptoms of C8-Th1 deficit with electrophysiological signs of postganglionic sensorimotor axon loss. 5 patients with only subjective symptoms who showed mild C8-Th1 sensory axon loss or no electrophysiological deficit at all were diagnosed with nonspecific TOS. A control group was also examined to obtain normal values for the CSA of the lower trunk and to check for the occurrence of any abnormality and sonographic Tinel sign. Descriptive statistics were applied to describe the age, age of onset of TOS symptoms in patients and CSA values of the lower trunk. Statistical significance was set at $p < 0.05$. GraphPad software was used for statistical calculations. A two-tailed unpaired t-test was used to test the difference between the age and CSA values of the control and patient groups. A two-tailed Fisher exact test was used to test for association between the clinical symptoms and signs suggestive of TOS and the presence of the wedge-sickle sign, and between the sonographic Tinel sign and the presence of the wedge-sickle sign. With respect to the clinical symptoms suggestive of TOS, the sensitivity and positive predictive value of the presence of the wedge-sickle sign and the sonographic Tinel sign were also calculated.

RESULTS

Carpal tunnel syndrome

The CSA of patients at both sites, and the WFR and PFR were significantly larger than those of the control group ($p < 0.001$ for all comparisons, Mann–Whitney U test). In the patient group, the CSA at the tunnel outlet and the PFR were significantly larger than the CSA at the tunnel inlet and the WFR, respectively ($p < 0.001$ for both comparisons, Wilcoxon matched pairs signed rank test). Furthermore, 27% of the hands showed CSA enlargement only at the outlet, and 13% only at the inlet. The optimal cut-off values for CSA-I, CSA-O, WFR, and PFR are shown in Table 1.

Table 1. Optimal cut-off values for CSA-I, CSA-O, WFR and PFR.

	CSA-I (mm²)	CSA-O (mm²)	WFR	PFR
Cut-off values	12,6	13,2	2	2
Sensitivity	80,4%	86,2%	68,2%	80%
Specificity	87,1%	93%	89,5%	89,6%
AUC	0,91	0,95	0,84	0,92

Cut-off, sensitivity and specificity values are rounded to the nearest decimal. CSA-I: cross-sectional area at the inlet; CSA-O: cross-sectional area at the outlet; WFR: wrist-toforearm CSA ratio; PFR: palm-to- forearm CSA ratio; AUC: area under the curve.

Table 2. shows the sensitivity, specificity, positive and negative predictive values, and accuracy for CSA-I, CSA-O, WFR, PFR and their combinations.

Table 2. Sensitivity, specificity, positive and negative predictive values and accuracy based on CSA enlargement at the outlet and inlet, abnormal WFR and PFR ratios, and their combinations.

	CSA-I	CSA-O	CSA-I+ CSA-O	WFR	PFR	WFR+PFR	All four
Sensitivity	79,7% (94/118)	84,8% (100/118)	94,9% (112/118)	68,6% (81/118)	78,8% (93/118)	89% (105/118)	96,6% (114/118)
Specificity	86,4 % (38/44)	93,2% (41/44)	81,8% (36/44)	90,9% (40/44)	90,9% (40/44)	81,8% (36/44)	70,5 % (31/44)
PPV	94% (94/100)	97,1 % (100/103)	93,3 % (112/120)	95,3% (81/85)	95,9% (93/97)	92,9% (105/113)	89,8% (114/127)
NPV	61,3% (38/62)	69,52% (41/59)	85,7% (36/42)	52% (40/77)	61,5% (40/65)	73,5% (36/49)	88,6% (31/35)
Accuracy	81,5% (94+38)/162)	87% (100+41)/162)	91,4% (112+36)/162)	74,7% (81+40)/162)	82,1% (93+40)/162)	87% (105+36)/162)	89,5% (114+31)/162)

Values are rounded to the nearest decimal. CSA-I: cross-sectional area at the inlet; CSA-O: cross-sectional area at the outlet; WFR: wrist-to-forearm CSA ratio; PFR: palm-toforearm CSA ratio; PPV: positive predictive value; NPV: negative predictive value; +: indicates and/or.

The point of maximum compression (flattening) within the tunnel was distal in all except for three hands. 3 patterns of distal compression were observed, in most cases there was a continuously decreasing LAPD from proximal to distal (Fig.2.). The jump in LAPD between the tunnel outlet and the distal tunnel (4–3) was 6.3% in the control and 127.3% in the patient group. Within the patient group the jump in LAPD at the tunnel inlet (1–2) was significantly smaller versus the jump at the tunnel outlet (4–3) ($p < 0.001$, Wilcoxon matched pairs signed rank test).

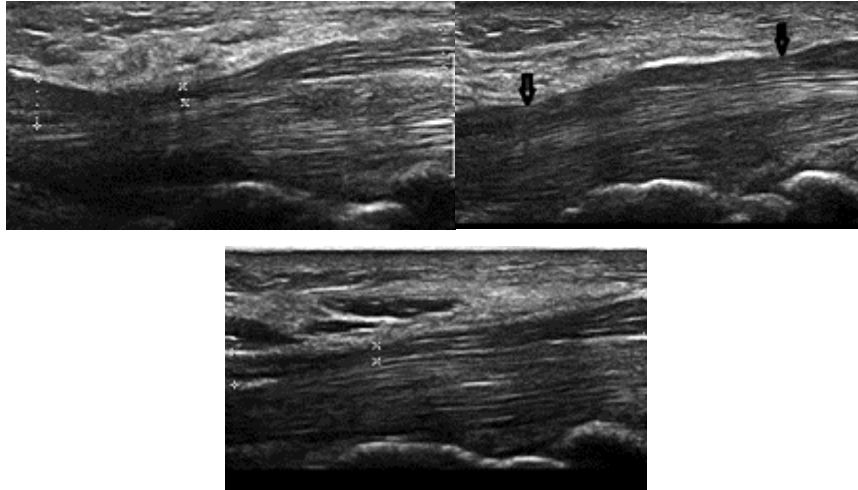


Fig. 2. Forms of distal compression in carpal tunnel syndrome. Abrupt focal LAPD decrease distally (left); distal LAPD drop in addition to the proximal compression (*right*); continuously decreasing LAPD from proximal to distal (middle).

Regarding the ten CTS patients with no electrophysiological deficit there was no significant difference between the cross sectional parameters in the control and patient group ($p > 0,10$ in all comparison, Mann–Whitney U test). There was no significant difference between CSA values at the outlet and inlet within the patient group either ($p = 0,06$ for CSA, $p = 0,10$ for PFR/WFR-re paired Wilcoxon test). Sensitivity, specificity, positive and negative predictive value and accuracy of the cross sectional parameters were well below compared to the electrophysiologically proven cases. LAPD jump at the border of outlet/distal tunnel (4-3) was 6,3% control and 111% in the patient group. Within the patient group the jump in LAPD at the tunnel inlet (1-2) was significantly smaller versus the jump at the tunnel outlet (4-3) ($p = 0,0016$, Wilcoxon matched pairs signed rank test). LAPD drop at the outlet (between site 4 and 3) was significantly greater in the patient group compared to the control group. ($p < 0,001$, Mann–Whitney U test).

Cubital and tarsal tunnel syndrome

On ultrasonographic assessment, extremely enlarged ulnar nerves were seen at the level of the medial epicondyle in both patients. The CSA_{max} value in patient 1. was 33 mm^2 on the left and 34 mm^2 on the right, and it was 43 mm^2 in patient 2. (norm: $< 10 \text{ mm}^2$). The CHR was 3,4 on the left and 3,9 on the right in patient 1 and 4,8 in patient 2. (norm: $< 1,4$). $LAPD_{max}$ in patient 1 was 6,9 mm on the left and 6,5 mm on the right, and it was 7,2 mm in patient 2. In patient 2 the nerve's fascicular structure was preserved, but individual fascicles were swollen. In the retrospectively analysed electrophysiologically confirmed 50 cubital tunnel patients the

mean CSA_{max} was 17.6 mm^2 (SD:5.86, min:6 mm^2 -max:33 mm^2), the CHR was 2.4 (SD: 0.7, min:1.3-max:5), and $LAPD_{max}$ was 4.2 mm (SD:1.14, min:1.9 mm-max:8.3 mm). In case 3 the tibial nerve was hypoechoic and extremely swollen with loss of fascicular structure immediately proximal to the tarsal tunnel. On longitudinal scans a spindle like hypoechoic swelling was seen. CSA increased from 16 to 66 mm^2 on the right, and from 14 to 26 mm^2 on the left (norm: <22 mm^2). An accessory flexor digitorum longus muscle was seen extending into the proximal tunnel on both sides, an anomaly known to be associated with tarsal tunnel syndrome.

Neurogenic TOS

In 19 patients the lower trunk of the brachial plexus was indented (compressed from the lateral direction) by a wedge-shaped, hyper-echoic fibromuscular structure at the medial edge of the middle scalene muscle, resulting in a sickle-shaped lower trunk (Fig. 3.). At the site of indentation, the lower trunk showed a complete loss of fascicular structure. The mean CSA of the lower trunk, measured at the site of compression, including the whole sickleshaped structure was $32.6 \pm 6.87 \text{ mm}^2$ (range: 20–50 mm^2) in the patient group and $16.76 \pm 3.9 \text{ mm}^2$ (range: 9–23 mm^2) in the control group. The difference between the two groups was statistically significant ($p < 0.0001$, two-tailed unpaired t-test). The association between clinical symptoms and signs suggestive of TOS and the presence of the wedge-sickle sign was statistically highly significant ($p < 0.0001$, two-tailed Fisher exact test). With respect to the clinical signs and symptoms suggestive of TOS the presence of the wedge-sickle sign had a sensitivity of 95% and a positive predictive value of 82.6% in our cohort. In 5 patients, the cranial end of the hyper-echoic fibromuscular structure was traced to a bony structure with posterior acoustic shadowing. All of these patients had either a cervical rib or an elongated C7 transverse process on radiography of the cervical spine. In the remaining patients, cranially the hyper-echoic fibromuscular structure gradually melted into the middle scalene muscle.

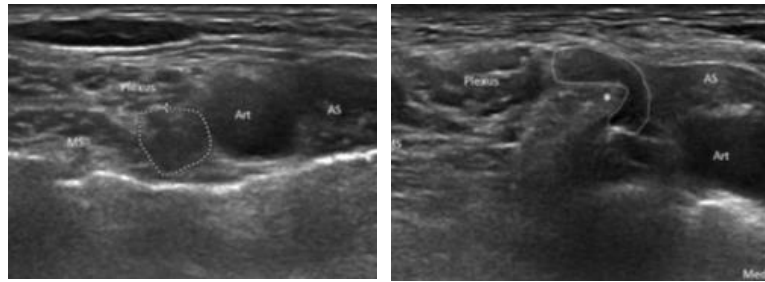


Fig. 3. 'wedge sickle sign'. Axial images reveal the lower trunk (dotted line) in the supraclavicular fossa. *Left: normal control. Right: The hyper-echoic pointed fibromuscular structure at the caudal medial aspect of the middle scalene muscle indents the lower trunk adjacent to the subclavian artery*
AS: anterior scalene muscle; MS: middle scalene muscle; Art: subclavian artery; asterisk (): indicates the hyper-echoic tip of the fibromuscular structure.*

In one patient (patient 20), a large bony cervical rib articulating with the first rib was found on the affected, right side. The anterior, articulating end of the cervical rib bulging into the supraclavicular fossa compressed the subclavian artery from the lateral direction and elevated and compressed the lower trunk of the brachial plexus from underneath. The association between the presence of the sonographic Tinel sign -which is a strong radiating electric-like pain and paresthesia in the arm provoked by pressing the transducer into the supraclavicular region- and the presence of the wedge-sickle sign was statistically highly significant ($p < 0.0001$, two-tailed Fisher exact test). With respect to the clinical symptoms of TOS, the presence of a supraclavicular Tinel sign had a sensitivity of 55% and a positive predictive value of 100% in our cohort.

Eight patients underwent surgery. In one patient, the whole middle scalene muscle was found to be hard and fibrotic, and scalenotomy was performed. In five patients, at the medial edge of the middle scalene muscle, a hard, fibrotic ligament indenting the lower trunk of the brachial plexus was found. The ligament was resected. Hourglass-like enlargement of the trunk was also observed. In one patient, the ligament at the medial edge of the middle scalene muscle was found attached to the elongated transverse process of the seventh cervical vertebra. The ligament was resected. In one patient, the ligament at the medial edge of the middle scalene muscle was attached to a cervical rib, but only the rib was removed. In all patients, pain and paresthesia in the arm decreased markedly after surgery, as reported by the patients. Long-term follow-up is pending.

CONCLUSIONS

Carpal tunnel syndrome

It has been shown experimentally that chronic nerve compression leads to endoneurial edema, perineurial and endoneurial thickening and to other ultrastructural changes with consequent nerve enlargement. In CTS, the swelling of the nerve at the tunnel inlet became the mainstay for the ultrasonographic diagnosis of CTS. It has been postulated that the swelling resulting from compression is translated to the site of least resistance, which explains why it is seen at the proximal edge of the retinaculum, at the tunnel inlet, where the nerve is relieved from pressure, rather than within the confined space of the tunnel. On the other hand such a relief and resulting swelling is expected at the distal edge of the retinaculum, at the tunnel outlet as well, an issue hitherto little addressed. We have shown in our cohort of idiopathic CTS patients that the median CSA at both the tunnel inlet and outlet is significantly larger than in the control group. Moreover in CTS patients the CSA at the outlet was significantly larger than the CSA at the inlet. For the diagnosis of CTS, the CSA at the outlet was associated with higher values for all diagnostic indicators (sensitivity, specificity, positive and negative predictive values, and accuracy) than the CSA at the inlet. When the CSA at the outlet and the inlet were both taken into account, sensitivity and accuracy increased by 15% and almost 10%, respectively, as opposed to the CSA at the inlet alone. These results confirm that swelling of the median nerve occurs at both ends of the tunnel in CTS and that swelling is even of greater degree at the tunnel outlet than at the inlet. Thus, the routine use of carpal tunnel outlet measurements is advocated.

It is an anatomical fact that the tunnel becomes progressively narrower from proximal to distal, and is the narrowest at the level of the hook of the hamate, at the distal insertion point of the flexor retinaculum. It has been demonstrated with *in vivo* segmental carpal tunnel pressure measurements in patients with idiopathic CTS that the site of the highest pressure corresponded to the area around the hook of hamate. We postulate that the greater degree of nerve enlargement at the tunnel outlet as opposed to the tunnel inlet is a sign of greater degree of compression in the distal than in the proximal portion of the tunnel in most patients. The point of maximum compression (flattening) within the tunnel was distal in 115 out of the 118 hands examined, moreover a significantly greater jump of diameter at the border of outlet/distal tunnel versus inlet/proximal tunnel was demonstrated in the patient group. Furthermore in the majority of CTS hands continuously decreasing LAPD, *i.e.* progressive flattening was observed from proximal to distal, which indicates progressively increasing

pressure and degree of compression within the tunnel from proximal to distal. Thus compression and pressure within the tunnel is higher in its distal portion, there is a greater relief from pressure at the tunnel outlet, than at the inlet. This has clinical relevance as an isolated or marked median nerve enlargement at the tunnel outlet may serve as a ‘whistleblower’ for the surgeon to perform extensive distal carpal tunnel release. The incomplete release of the distal portion of the flexor retinaculum may lead to incomplete alleviation of symptoms.

In the 10 electrophysiologically negative CTS cases (12 hands), there was no significant difference between the patient and control group in regard to the the cross sectional parameters. On the other hand LAPD jump at the border of outlet/distal tunnel was significantly greater in the patient, than in the control group, and LAPD jump at the border of outlet/distal tunnel was significantly greater than LAPD jump at the border of inlet/proximal tunnel within the patient group. Diagnostic indicators (sensitivity, specificity, positive and negative predictive values, and accuracy) of the cross sectional parameters showed considerably lower values as opposed to the electrophysiologically proven cases, but longitudinal scans confirmed compression in these patients as well. Scanning performed as far as the tunnel outlet and visual evaluation is of utmost importance in this patient group, because compression should be searched distally.

Cubitalis tunnel and tarsal syndrome

Pathophysiological events in compressive neuropathies may lead to a drastic, tumor-like nerve enlargement in some individuals. We present three cases of entrapment neuropathies where the degree of the fusiform hypoechoic nerve swelling (a 3–4-fold increase in nerve size) was unusual for entrapment neuropathies, creating a diagnostic challenge at first. A large fusiform swelling of peripheral nerves may also be caused by other conditions like posttraumatic neuromas, pseudoneuromas, inflammatory peripheral nerve lesions and peripheral nerve sheath tumors. Nerve tumours may also occur at entrapment sites, but this group could be excluded based on certain ultrasonographic, clinical and electrophysiological signs. A rare tumour, intraneural perineurioma typically involves a long nerve segment with preserved fascicular echotexture, which was particularly considered in one of the patients. However, intraneural perineurioma usually occurs at an early age in the sciatic nerve or its branches, and causes early and severe motor deficit, which was not the case in our patient. An important conclusion is that ultrasonography should not play an exclusive role in the

diagnosis of peripheral nerve lesions; clinical, electrophysiological and operative findings should all be taken into account for a correct diagnosis.

Neurogenic TOS

Based on our observations neurogenic TOS is more common than previously thought. HRUS and surgically proven cases urged us to direct our focus on this entity, even in cases with non specific symptoms. Roos, based on his surgical and cadaver studies identified 10 different types of fibromuscular bands, that may cause compression of the Th1 root or the lower trunk in the supraclavicular fossa. The observed distinctive ultrasonographic sign, the wedge-sickle sign, which is a fibromuscular structure with a pointed, hyper-echoic tip along the caudal medial edge of the middle scalene muscle, may correspond to one of these ligaments.

Five patients were diagnosed with nonspecific TOS, a controversial category with subjective symptoms such as pain and paresthesia in the arm with no clinical deficit. The association of the wedge-sickle sign could also be observed in 4 patients of the non-specific TOS group. Pre-surgical identification of the fibromuscular structure as the cause of compression of the lower trunk is especially important in this group, since in more progressed stages proximo-distal axonal regrowth is unlikely because of the long distance.

PUBLICATONS

Publications related to the thesis

Csillik A, Bereczki D, Bora L, Arányi Z.: The significance of ultrasonographic carpal tunnel outlet measurements in the diagnosis of carpal tunnel syndrome. *Clin Neurophysiol* 2016; 127:3516-3523.

Csillik A, Tóth M, Arányi Z.: Tumour-like giant nerves in entrapment neuropathies. *Clin Neurophysiol* 2017; 129(3):555-557.

Arányi Z, Csillik A, Böhm J, Schelle T.: Ultrasonographic identification of fibromuscular bands associated with neurogenic thoracic outlet syndrome: the 'wedge-sickle' sign. *Ultrasound Med Biol* 2016; 42:2357-2366.

Other publications

Csillik Anita, Pozsonyi Zoltán, Soós Krisztina, Balogh István, Bodó Imre, Arányi Zsuzsanna: Transthyretin familiáris amyloid polyneuropathia - három magyarországi eset ritka mutációkkal (His88Arg és Phe33Leu). *Ideggyógyászati Szemle* 2016; 69(7-8).

Arányi Z, Csillik A, Dévay K, Rosero M, Barsi P, Böhm J, Schelle T.: Ultrasonographic identification of nerve pathology in neuralgic amyotrophy: Enlargement, constriction, fascicular entwinement, and torsion. *Muscle Nerve* 2015; 52:503-511.

Arányi Z, Csillik A, Dévay K, Rosero M.: Ultrasonographic demonstration of intraneural neovascularization after penetrating nerve injury. *Muscle Nerve* 2018; 57 (6):994-999.